Effect of Contact between Myoblasts on Making Orientation of Cells under Shear Flow Field

*Shigehiro Hashimoto[1] Michitaka Sakai[1] Hiroki Yonezawa[1] and Yuji Endo[1]

[1] *Kogakuin University*

Abstract[1]

The effect of contact between cells on forming orientation of cells under the shear flow field has been investigated in vitro. To create a Couette type of the shear flow, the culture medium was sandwiched with a constant gap between parallel walls: a lower stationary culture disk, and an upper rotating disk. The wall shear stress (2 Pa) on the lower culture disk was controlled by the rotating speed of the upper disk. Myoblasts (C2C12: mouse myoblast cell line) were used in the test. After cultivation without flow for 24 hours for adhesion of cells on the lower plate, the constant wall shear stress was continuously applied on cells for 7 days in the incubator. The behavior of each cell was traced at the time-lapse images observed by an inverted phase contrast microscope placed in an incubator. The experimental results quantitatively show that increase of the contact region between cells affects forming perpendicular orientation of cells against the main flow direction.

Keywords: *Biomedical Engineering, Interaction between Cells, Wall Shear Stress, C2C12 and Orientation.*

1. Introduction

Biological cells orient in the tissue. Orientation is related to the function of the tissue. The process of forming cell orientation in a tissue depends on the surrounding environment (Lecaudey, 2006). The mechanical force field is one of the environments (Grossi, 2008). The effects of the shear flow on the endothelial cells exposed to the blood flow on the inner surface of the vessel wall (Chen, 2010) were investigated in many studies (Conway, 2013). Endothelial cells form orientation on the inner surface of the blood vessel wall. The orientation is parallel to the blood flow direction. In the previous study with the vortex flow by the swinging plate *in vitro*, C2C12 (mouse

* Shigehiro Hashimoto, Mechanical Engineering, Kogakuin University, Tokyo, 192-0015, Japan (at13351@g.kogakuin.jp). This article was presented at IMCIC2021 in March 2021.
[1] The authors are grateful to Professor Richard Magin for his proofreading of this article.

myoblast cell line) oriented perpendicular to the direction of the flow, although HUVEC (human umbilical vein endothelial cell) oriented along the streamline of the flow (Hashimoto, 2011).

The alignment of each cell also depends on those of adjacent cells. The alignment of the cell tends to create parallel orientations according to those of adjacent cells. In the present study, the effect of interaction between cells on forming orientation of cells under the shear flow field has been investigated *in vitro*.

2. Methods

2.1. Shear Flow Device

In the present study, a Couette type shear flow device has been used (Figure 1). The medium is sheared between a rotating wall and a stationary wall. The stationary wall is the bottom of the culture dish (diameter 60 mm).

The shear rate (γ) in the medium is calculated by Equation (1) in the device.

$$\gamma = b\,\omega / d \qquad (1)$$

In Equation (1), ω is the angular velocity [rad s^{-1}], and d is the distance [m] between the wall of the moving disk and the wall of stationary plate. Between the parallel walls, d is constant.

The angular velocity ω (22 rad s^{-1}) was controlled by the stepping motor. In the observation area of the microscope, b varies between 17 mm and 18 mm. The distance d, which was measured by the positions of the focus of the walls at the microscope, was 0.29 mm. The shear rate (γ) is set at 1.3×10^{3} s^{-1} in the present experiment by adjustment of these parameters.

The shear stress (τ [Pa]) is calculated by Equation (2).

$$\tau = \eta\,\gamma \qquad (2)$$

In Equation (2), η is the viscosity [Pa s] of the medium. Using the viscosity of the medium of 1.5×10^{-3} Pa s (measured by a cone and plate viscometer at 310 K), the shear stress τ is calculated as 2.0 Pa. The rotating disk device is mounted on the stage of the inverted phase contrast microscope placed in the incubator. The device allows microscopic observation of cells cultured on the stationary wall during exposure to the shear flow.

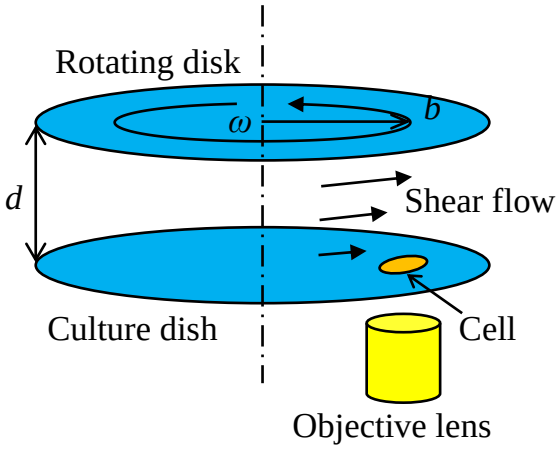

Figure 1: Shear flow between rotating disk and stationary dish.

2.2. Cell Culture

C2C12 (mouse myoblast cell line originated with cross-striated muscle of C3H mouse, passage between eight and ten) was used in the test. Cells were cultured in the Dulbecco's Modified Eagle's medium (D-MEM): containing 10% of the decomplemented fetal bovine serum (FBS), sodium hydrogen carbonate ($NaHCO_3$), and 1% of penicillin/ streptomycin.

The cells were seeded on the bottom of the dish at a density of 3000 cells/cm^2. To adhere the cells to the bottom of the culture dish, the cells were cultured in the incubator for 24 hours without flow stimulation (without rotating the disk).

After the incubation for 24 hours, the cells were continuously sheared with the rotating disk for 7 days in the incubator at the constant rotating speed without the medium exchange. The constant speed was preset for each test to keep the designed shear stress.

2.3. Image Analysis

The time-lapse microscopic images were taken every thirty minutes during the cultivation. The contour of each cell adhered on the stationary plate of the scaffold was traced (Figure 2), and was approximated to the ellipsoid.

The angle (0 degree < θ < 180 degree) between the longitudinal axis of the cell and the flow direction was measured at the microscopic image of each cell. The alignment of each cell was traced for 24 hours under the continuous shear flow stimulation.

The length of the contact line (x) between cells was measured on the image (Figure 3). The length ratio R is calculated by Equation (3).

$$R = x / S \qquad (3)$$

S is the peripheral length of the smaller cell.

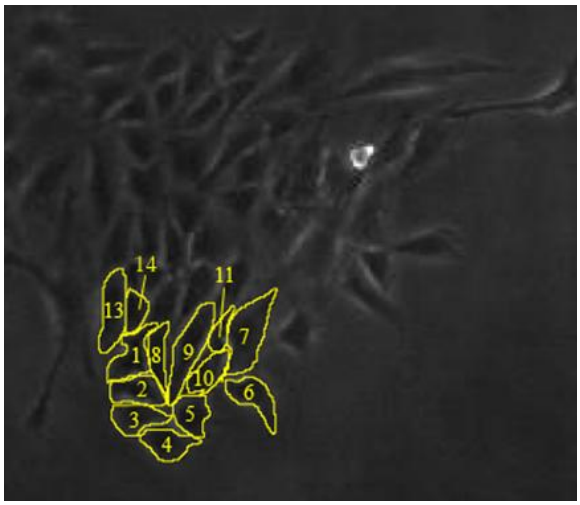

Figure 2a: Traced single cells (1-14) in area A.

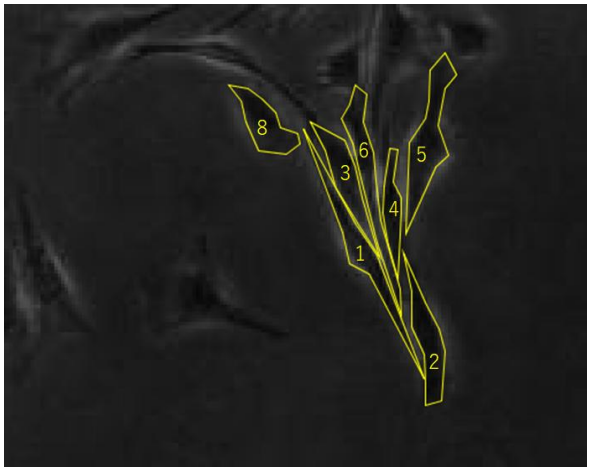

Figure 2b: Traced single cells (1-8) in area B.

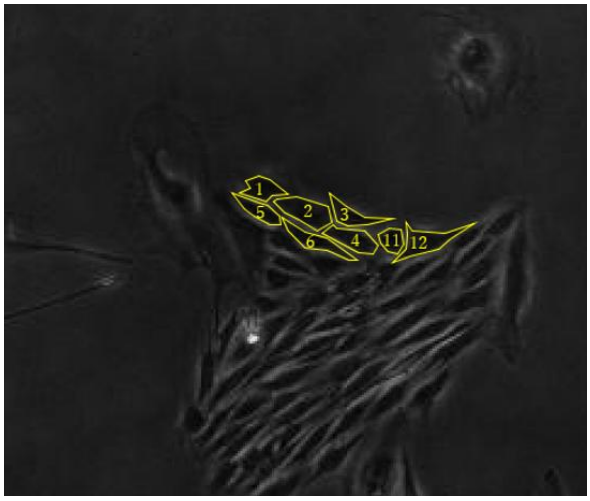

Figure 2c: Traced single cells (1-12) in area C.

3. Results

Myoblasts showed every activity during cultivation under the continuous constant wall shear field: migration, exfoliation, deformation, division, and fusion to make myotubes. Figure 4 exemplifies tracings of the angle (θ) between the longitudinal axis of the cell and the flow direction for 24 hours in the colony in the area B. Every cell in Figure 4 approaches to 90 degrees, which indicates forming orientation perpendicular to the flow direction. The

length of the contact line (x) between cells varies during the period (Figure 5). In the following figures, the contact between cells is evaluated by the length ratio.

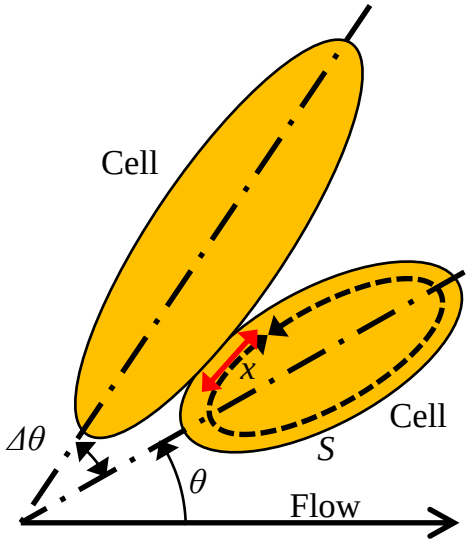

Figure 3: Contact between cells.

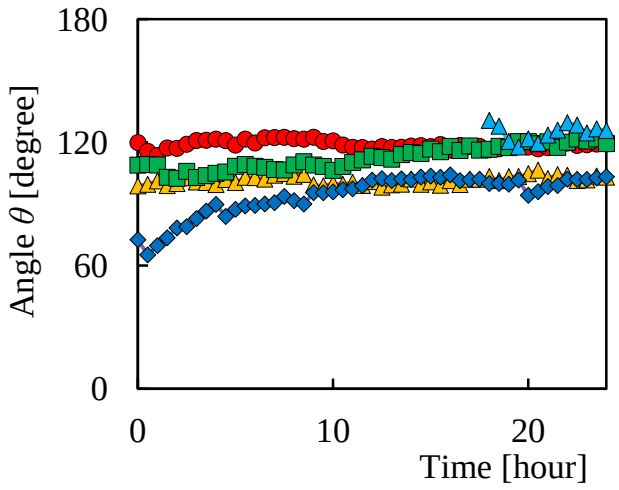

Figure 4: Tracings of angle θ of cell

Figure 6 shows the angle between cells ($\Delta\theta$) in relation to the length ratio (R) in the colony in the area A (Figure 2a). Figure 7 shows the angle between cells ($\Delta\theta$) in relation to the length ratio (R) in the colony in the area B (Figure 2b). Figure 8 shows the angle between cells ($\Delta\theta$) in relation to the length ratio (R) in the colony in the area C (Figure 2c). The regression lines

are added to the data between cells, which has wider variation of the length ratio (R). The correlation coefficient (r) was calculated for each regression line.

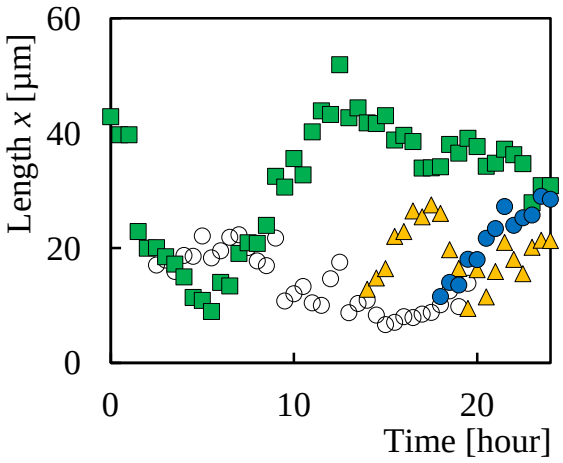

Figure 5: Tracings of contact length x between cells.

Regression lines in Figures 6a-6e have negative slopes. The correlation coefficients (r) are in the range between 0.31 and 0.62 in Figures 6a-6d. When the angle between cells ($\Delta\theta$) is larger than 30 degrees, the angle $\Delta\theta$ tends to decrease with the length ratio (R). When the angle $\Delta\theta$ is smaller than 30 degrees, on the other hand, the angle does not decrease every time (Figure 7). In some cases, the angle $\Delta\theta$ increases with the length ratio (R) (Figure 7g, Figure 7b, Figure 8a, Figure 8b).

Figure 7 shows the angle ($\Delta\theta$) in relation to the length ratio (R), when the longitudinal direction of each cell is perpendicular to the wall shear stress direction. Slopes between $\Delta\theta$ and R are very small. Angles ($\Delta\theta$) are maintained smaller than 30 degrees. The parallel position between cells is kept in the direction perpendicular to the flow.

Figure 8 shows the angle ($\Delta\theta$) in relation to the length ratio (R), when the longitudinal direction of each cell is parallel to the wall shear stress direction. When the angle between cells ($\Delta\theta$) is larger than 30 degrees, the angle $\Delta\theta$ tends to decrease with the length ratio (R) (Figure 8a, Figure 8b).

Although angles ($\Delta\theta$) smaller than 30 degrees are maintained, the angle $\Delta\theta$ increases with the length ratio (R) (Figure 8b) in some cases.

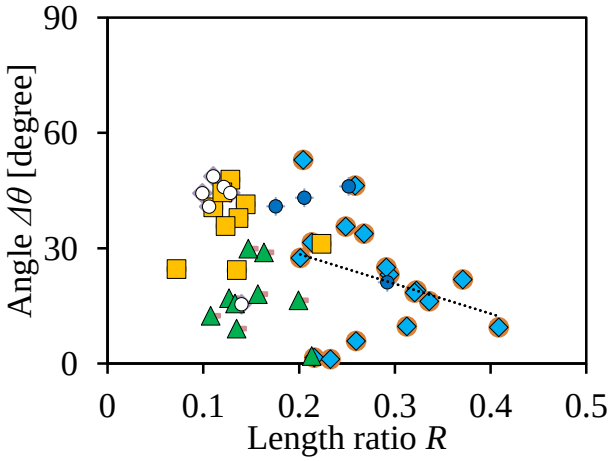

Figure 6a: Length ratio R vs. angle $\Delta\theta$ in contact of cell 1 with cell 14 (open circle), cell 8 (blue circle), cell 13 (square), cell 12 (triangle), and cell 2 (rhombus): dotted line, regression line between cell 1 and 2 ($\Delta\theta = -77\ R + 44$): correlation coefficient $r = 0.31$.

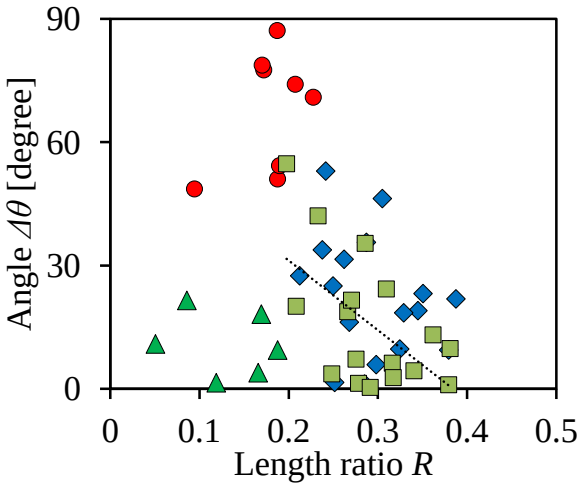

Figure 6b: Length ratio R vs. angle $\Delta\theta$ in contact of cell 2 with cell 8 (circle), cell 3 (square), cell 12 (triangle), and cell 1 (rhombus): dotted line, regression line between regression line between cell 2 AND 3 ($\Delta\theta = 170\ R + 65$): correlation coefficient $r = 0.58$.

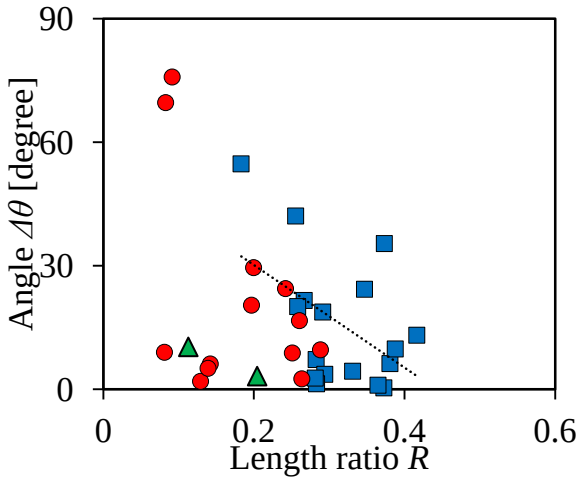

Figure 6c: Length ratio R vs. angle $\Delta\theta$ in contact of cell 3 with cell 8 (circle), cell 2 (square), and cell 4 (triangle): dotted line, regression line between cell 2 and 3 ($\Delta\theta = -125\ R + 55$): correlation coefficient $r = 0.48$.

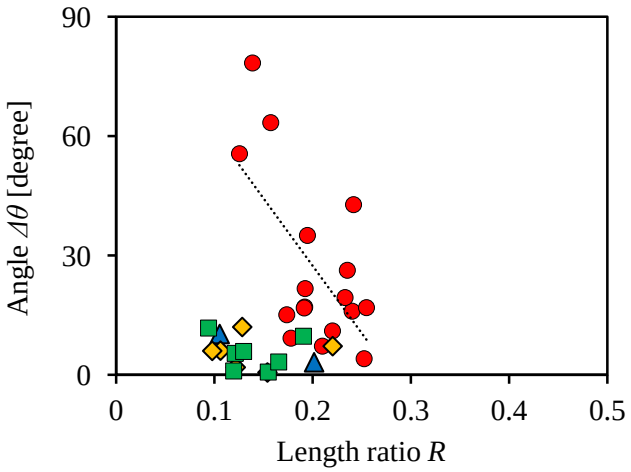

Figure 6d: Length ratio R vs. angle $\Delta\theta$ in contact of cell 4 with cell 5 (circle), cell 9 (square), cell 3 (triangle), and cell 8 (rhombus): dotted line, regression line between cell 4 and 5 ($\Delta\theta = -339\ R + 95$): correlation coefficient $r = 0.62$.

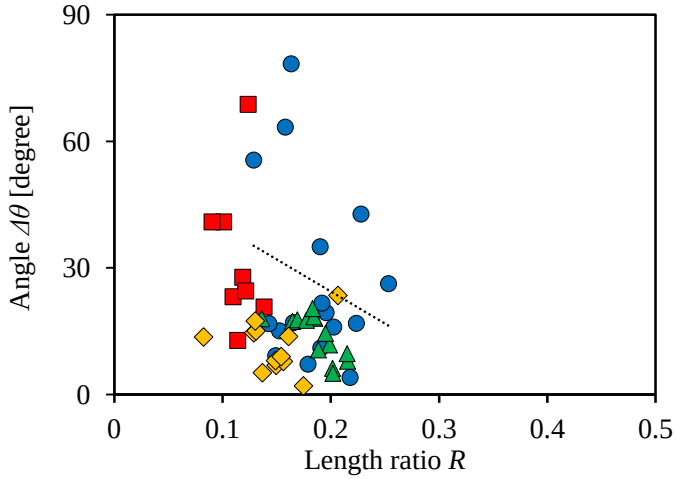

Figure 6e: Length ratio R vs. angle $\Delta\theta$ in contact of cell 5 with cell 4 (circle), cell 6 (square), cell 9 (triangle), and cell 10 (rhombus): dotted line, regression line between cell 4 and 5 ($\Delta\theta = -152\ R + 55$): correlation coefficient $r = 0.24$.

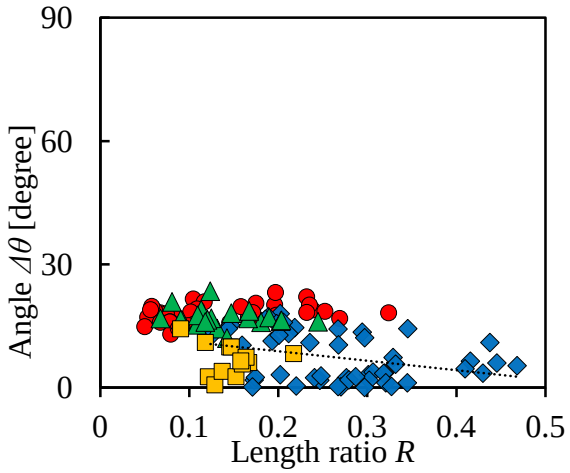

Figure 7a: Length ratio R vs. angle $\Delta\theta$ in contact of cell 1 with cell 2 (circle), cell 8 (square), cell 6 (triangle), and cell 3 (rhombus): dotted line, regression line between cell 1 and 3 ($\Delta\theta = -23\ R + 13$): correlation coefficient $r = 0.33$.

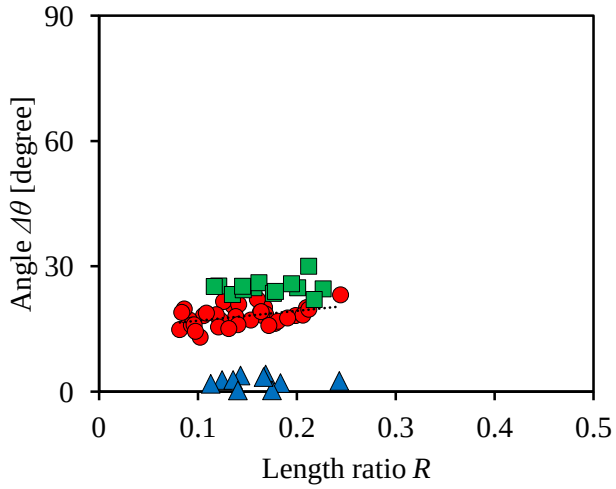

Figure 7b: Length ratio R vs. angle $\Delta\theta$ in contact of cell 2 with cell 1 (circle), cell 5 (square), and cell 6 (triangle): dotted line, regression line between cell 1 and 2 ($\Delta\theta = 23\ R + 15$): correlation coefficient $r = 0.44$.

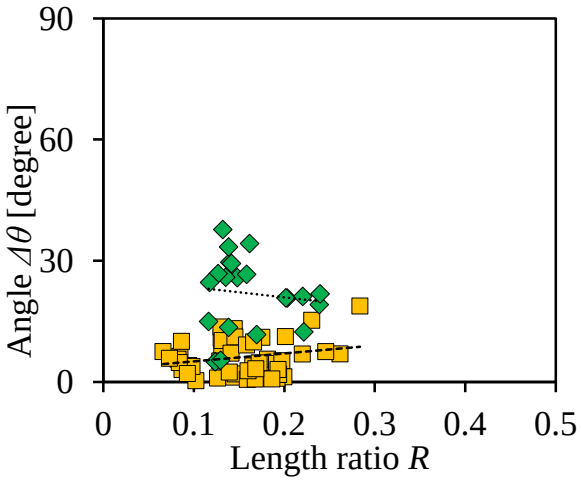

Figure 8a: Length ratio R vs. angle $\Delta\theta$ in contact of cell 8 with cell 1 with cell 2 (square), and cell 5 (rhombus): dotted line, regression line between cell 1 and 5 ($\Delta\theta = -25\ R + 26$): correlation coefficient $r = 0.11$: broken line, regression line between cell 1 and 2 ($\Delta\theta = 20\ R + 3$): correlation coefficient r = 0.23.

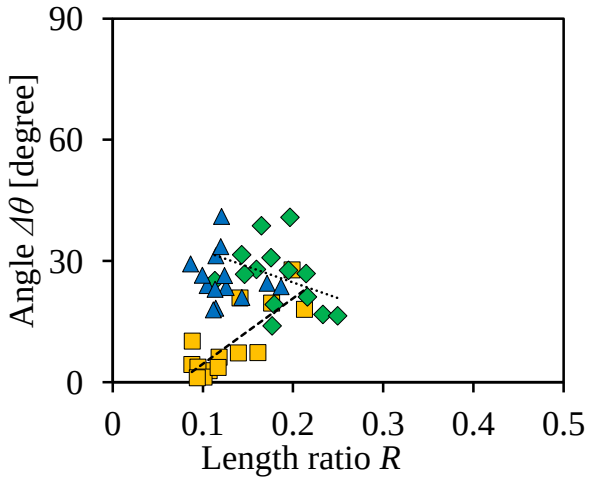

Figure 8b: Length ratio R vs. angle $\Delta\theta$ in contact of cell 8 with cell 7 (square), cell 12 (triangle), and cell 10 (rhombus): dotted line, regression line between cell 8 and 10 ($\Delta\theta = -77\ R + 40$: correlation coefficient r = 0.36: broken line, regression line between cell 7 and 8 ($\Delta\theta = 162\ R - 12$): correlation coefficient r = 0.80.

4. Discussion

To study on the orientation of cells, the orientation should be evaluated quantitatively by the parameter. The shape of each C2C12 adhered on the culture plate can be approximated to the ellipsoid. In the previous study, the distribution of the direction of the longitudinal axis of each ellipsoid has been measured (Hashimoto, 2020b). Under the wall shear stress, a cell shows the following responses: elongation, tilting to the streamline, migration, deformation to be rounded, division, and exfoliation from the wall of the scaffold. In the Poiseuille type of flow, the shear rate depends on the distance from the wall: zero at the center of the flow-path, and the highest value at the wall. In the Couette type of flow, on the other hand, the shear rate is constant regardless of the distance from the wall (Hashimoto, 2019).

The experimental results show that each single cell tends to align parallel to the flow direction under shear stress of 2 Pa in the previous study (Hashimoto, 2020b). The mean direction of cells in some colonies of

C2C12 tends to align perpendicular to the flow direction. Because of the interaction of cells, the direction of the cell depends on that of the neighbor cell. The myoblasts fuse to form the myotubes. The results would be applied to create orientation of myotubes in an engineered tissue. The experimental methods to control the shear field of the medium in the flow would be applied to the acceleration technique to create orientation of cells *in vitro*.

When the angle between cells ($\Delta\theta$) is larger than 30 degrees, the contact between cells affect the angle change. The smaller cell tends to align parallel to the neighbor cell (Endo, 2020). When the angle between cells is small, the parallel position between cells is maintained. In these processes, the orientation of cells perpendicular to the flow direction can be formed in the colony.

The interaction between cells governs the behavior of each cell. The orientation of each cell depends on the orientation of the neighbor cell. Myoblasts tend to migrate to the oblique direction under the shear stress field of 1.5 Pa (Hashimoto, 2020a). The effect of shear flow on cells depends on the cell types. The dependency might be applied to the cell sorting technology (Lima, 2018) (Islamzada, 2019). The quantitative relationships between the shear stress and the cell orientation might be applied to tissue technology to control of cells *in vitro*.

In the tissue technology, orientation of cells was controlled by the design of the scaffold *in vitro*. Alignment of fibers of the scaffold was controlled by the electrospinning technique (Murugan, 2007). 3D-printing technology was applied to create orientation of cells (Wu, 2019). The Micro-robotic technique was applied to the cell manipulation to control orientation of each cell (Liu, 2009).

Endothelial cells are exposed to the shear flow in the blood vessels *in vivo*. The shear flow affects vessel wall (Xu, 2016) (Arzani, 2018) and clot formation (Tosenberger, 2015). The effects of shear flow on endothelial cells were investigated in the previous studies (Ostrowski, 2014) (Steward Jr, 2015) (Nagel, 1994). Cells are exfoliated under the shear flow at the wall shear stress higher than 2 Pa (Hashimoto, 2013) (Sato, 2013) (Hino, 2016). A biological cell shows passive and active responses in an

environment (Ostrowski, 2014). While the flow enhances the cell migration to the downstream, a cell migrates to adapt to the shear field. While the strong stimulation above the threshold damages the cell, the stimulation below the threshold remains in the cell as a memory for the response in the next step (Steward Jr, 2015) (Nagel, 1994). The hysteresis effect governs the active response of the cell. The expanded version of this study was presented at the FEDSM conference in August 2021 (Hashimoto, 2021).

5. Conclusions

The experimental results quantitatively show that increase of the contact region creates parallel orientation between cells. The contact region between cells affects creating perpendicular orientation of cells against the main flow direction.

6. Acknowledgments

The authors thank Mr. Hiroki Eri for his assistance of the experiment.

References

Arzani, A., & Shadden, S. C. (2018). Wall Shear Stress Fixed Points in Cardiovascular Fluid Mechanics. *Journal of Biomechanics, 73*, 145-152.

Chen, Z. Peng, I. C., Cui, X., Li, Y. S., Chien, S., & Shyy, J. Y. J. (2010). Shear Stress, SIRT1, and Vascular Homeostasis. *Proceedings of the National Academy of Sciences*, 107(22), 10268-10273.

Conway, D. E., Breckenridge, M. T., Hinde, E., Gratton, E., Chen, C. S., & Schwartz, M. A. (2013). Fluid Shear Stress on Endothelial Cells Modulates Mechanical Tension across VE-Cadherin and PECAM-1. *Current Biology, 23*, 1024-1030.

Endo, Y., Hashimoto, S., Toma, S., Asahino, A., & Yoshinaka, K. (2020). Cultured Myoblasts Orientation under Couette Type of Shear Flow between Parallel Disks: Fusion and Division. *Proc. 24th World Multi-Conference on Systemics Cybernetics and Informatics, 2*, 1-6.

Grossi, A., Karlsson, A. H., & Lawson, M. A. (2008). Mechanical Stimulation of C2C12 Cells Increases M-calpain Expression, Focal Adhesion Plaque Protein Degradation. *Cell Biology International, 32*, 615-622.

Hashimoto, S., & Okada, M. (2011). Orientation of Cells Cultured in Vortex Flow with Swinging Plate In Vitro. *Journal of Systemics Cybernetics and Informatics, 9(3)*, 1-7.

Hashimoto, S., Sato, F., Hino, H., Fujie, H., Iwata, H., & Sakatani, Y. (2013). Responses of Cells to Flow In Vitro. *Journal of Systemics Cybernetics and Informatics, 11(5)*, 20-27.

Hashimoto, S., Sugimoto, H., & Hino, H. (2019). Effect of Couette Type of Shear Stress Field with Axial Shear Slope on Deformation and Migration of Cell: Comparison between C2C12 and HUVEC. *Journal of Systemics Cybernetics and Informatics, 17(2)*, 4-10.

Hashimoto, S., Shimada, K., & Endo, Y. (2020a). Migration of Cell under Couette Type Shear Flow Field between Parallel Disks: After and Before Proliferation. *Proc. 11th International Multi-Conference on Complexity Informatics and Cybernetics, 2*, 19-24.

Hashimoto, S. (2020b). Behavior of Myoblast under Shear Stress in Couette Type of Flow. *Proc. ASME Fluids Engineering Division Summer Meeting*, FEDSM2020-2075, 1-7.

Hashimoto, S., & Yokomizo, T. (2021). Tracings of Interaction between Myoblasts under Shear Flow In Vitro. *Proc. ASME Fluids Engineering Division Summer Meeting*, FEDSM2021-65203, 1-9.

Hino, H., Hashimoto, S., Takahashi, Y., & Nakano, S. (2016). Design of Cross Type of Flow Channel to Control Orientation of Cell. *Proc. 20th World Multi-Conference on Systemics Cybernetics and Informatics, 2*, 117-122.

Islamzada, E., Matthews, K., Guo, Q., Santoso, A., Scott, M. D., & Ma, H. (2019). Deformability Based Sorting of Stored Red Blood Cells Reveals Donor-Dependent Aging Curves. *Blood, 134, Supplement 1*, 3694.

Lecaudey, V., & Gilmour, D. (2006). Organizing Moving Groups during Morphogenesis. *Current Opinion in Cell Biology, 18*, 102-107.

Lima, T. I., & Silveira, L. R. (2018). A Microplate Assay for Measuring Cell Death in C2C12 Cells. *Biochemistry and Cell Biology, 96(5)*, 702-706.

Liu, X., & Sun, Y. (2009). Visually Servoed Orientation Control of Biological Cells in Microrobotic Cell Manipulation. In: Khatib, O., Kumar, V., & Pappas, G. J. (eds), Experimental Robotics, *The 11th International Symposium STAR, 54*, 179-187.

Murugan, R., & Ramakrishna, S. (2007). Design Strategies of Tissue Engineering Scaffolds with Controlled Fiber Orientation. *Tissue Engineering, 13(8)*, 1845-1866.

Nagel, T., Resnick, N., Atkinson, W. J., Dewey Jr C. F., & Gimbrone Jr, M. A. (1994). Shear Stress Selectively Upregulates Intercellular Adhesion Molecule-1 Expression in Cultured Human Vascular Endothelial Cells. The Journal of Clinical Investigation, 94(2), 885-891.

Ostrowski, M. A., Huang, N. F., Walker, T. W., Verwijlen, T., Poplawski, C., Khoo, A. S., Cooke, J. P., Fuller, G. G., & Dunn, A. R. (2014). Microvascular Endothelial Cells Migrate Upstream and Align Against the Shear Stress Field Created by Impinging Flow. *Biophysical Journal, 106(2)*, 366-374.

Sato, F., Hashimoto, S., Yasuda, T., & Fujie, H. (2013). Observation of Biological Cells in Rhombus Parallelepiped Flow Channel. *Proc. 17th World Multi-Conference on Systemics Cybernetics and Informatics, 1*, 25-30.

Steward Jr, R., Tambe, D., Hardin, C. C., Krishnan, R., & Fredberg, J. J. (2015). Fluid Shear, Intercellular Stress, and Endothelial Cell Alignment. *American Journal of Physiology–Cell Physiology, 308*, C657-C664.

Tosenberger, A., Ataullakhanov, F., Bessonov, N., Panteleev, M., Tokarev, A. A., & Volpert, V. (2015). Modelling of Platelet–fibrin Clot Formation in Flow with a DPD–PDE Method. *Journal of Mathematical Biology, 72(3)*, DOI: 10.1007/s00285-015-0891-2

Wu, F., Zheng, J., Li, Z., & Liu, M. (2019). Halloysite Nanotubes Coated 3D Printed PLA Pattern for Guiding Human Mesenchymal Stem Cells (hMSCs) Orientation. *Chemical Engineering Journal, 359*, 672-683.

Xu, L., Sugawara, M., Tanaka, G., Ohta, M., Liu, H., & Yamaguchi, R. (2016). Effect of Elasticity on Wall Shear Stress Inside Cerebral Aneurysm at Anterior Cerebral Artery. *Technology and Health Care, 24*, 349-357.